Clinical & Experimental Immunology
The Journal of Translational Immunology

Clinical and Experimental Immunology ORIGINAL ARTICLE doi:10.1111/j.1365-2249.2010.04234.x

Use of bioluminescence imaging to track neutrophil migration and its inhibition in experimental colitis

C. T. Murphy,* G. Moloney,*† L. J. Hall,* A. Quinlan,* E. Faivre,* P. Casey,* F. Shanahan,* S. Melgar*† and K. Nally*

*Alimentary Pharmabiotic Centre, University College Cork, National University of Ireland, Cork, Ireland, and †Immuno-Inflammation, CEDD, GlaxoSmithKline, Stevenage, UK

Accepted for publication 29 June 2010
Correspondence: Professor F. Shanahan, Department of Medicine/Alimentary Pharmabiotic Centre, 5th Floor, Biosciences Institute, Western Road, University College Cork, Cork, Ireland.
E-mail: f.shanahan@ucc.ie

Summary

Inflammatory bowel disease (IBD) is associated with neutrophil infiltration into the mucosa and crypt abscesses. The chemokine interleukin (IL)-8 [murine homologues (KC) and macrophage inflammatory protein (MIP)-2] and its receptor CXCR2 are required for neutrophil recruitment; thus, blocking this engagement is a potential therapeutic strategy. In the present study, we developed a preclinical model of neutrophil migration suitable for investigating the biology of and testing new drugs that target neutrophil trafficking. Peritoneal exudate neutrophils from transgenic β-actin-*luciferase* mice were isolated 12 h after intraperitoneal injection with thioglycollate, and were assessed phenotypically and functionally. Exudate cells were injected intravenously into recipients with dextran sodium sulphate (DSS)-induced colitis followed by bioluminescence imaging of whole-body and *ex vivo* organs at 2, 4 and 16–22 h post-transfer. Anti-KC antibody or an isotype control were administered at 20 μg/mouse 1 h before transfer, followed by whole-body and organ imaging 4 h post-transfer. The peritoneal exudate consisted of 80% neutrophils, 39% of which were CXCR2$^+$. *In vitro* migration towards KC was inhibited by anti-KC. *Ex vivo* bioluminescent imaging showed that neutrophil trafficking into the colon of DSS recipients was inhibited by anti-KC 4 h post-cell transfer. In conclusion, this study describes a new approach for investigating neutrophil trafficking that can be used in preclinical studies to evaluate potential inhibitors of neutrophil recruitment.

Keywords: bioluminescence imaging, DSS colitis, inflammatory bowel disease, neutrophils

Introduction

Polymorphonuclear (PMN) neutrophil transmigration across the mucosa and into intestinal crypts is a major characteristic of the inflammatory bowel diseases (IBD), Crohn's disease (CD) and ulcerative colitis (UC). Excessive or unchecked neutrophil recruitment can lead to tissue damage, due mainly to the persistent release of harmful inflammatory cytokines, reactive oxygen species and proteases by the infiltrated cells [1]. In active IBD, histological evidence of high-density neutrophil accumulation in the intestinal lumen correlates directly with epithelial injury and clinical disease activity [2]. Therefore, targeting neutrophil influx is a potential therapeutic strategy for IBD.

The CXC chemokines, human interleukin-8 (IL-8/CXCL8) and the murine functional homologues keratinocyte-derived chemokine (KC/CXCL1) and macrophage inflammatory protein-2 (MIP-2/CXCL2), are neutrophil chemoattractants that orchestrate their activation and recruitment from the blood into sites of infection, inflammation and injury by promoting endothelial adhesion and transmigration [3]. Their biological effects are mediated by binding to two high-affinity receptors, CXCR1 and CXCR2 [4]. CXCR2 has proved to be a potent mediator of PMN recruitment in preclinical models of arthritis [5], allergy [6], respiratory disease [7] and ulcerative colitis [8]. Increased mucosal expression of these chemokine receptors and their ligands in IBD explains the massive influx of leucocytes in active disease. The up-regulation of IL-8 in the colonic mucosa of IBD patients [9,10] correlates well with the histological degree of inflammation and chemokine mRNA expression [11,12]. The pivotal involvement of keratinocyte-derived chemokine (KC) and macrophage inflammatory protein-2 (MIP-2) in PMN infiltration into

inflammatory sites is also well documented [13,14]. Furthermore, a marked increase in KC and MIP-2 have been reported in colons of mice with acute phase dextran sulphate sodium (DSS)-induced colitis [15].

Traditional methods used to track neutrophil recruitment, such as static histological analysis of fixed tissues following adoptive transfer of dye-labelled cells, do not provide temporal or spatial information within the physiological environment of lymphoid tissues [16]. While white cell scintigraphy has been used to study neutrophil migration in both preclinical and clinical IBD studies [17,18], there are well-recognised disadvantages associated with radiotracers including the adverse effect on cell viability, radioactive decay and poor resolution [19]. In this study, a novel method to track neutrophil recruitment is described, involving bioluminescence imaging of adoptively transferred luciferase-expressing peritoneal exudate cells. We also investigated the blocking effect that an anti-KC antibody may have on neutrophil homing to the inflamed intestines of mice with DSS-induced colitis. The results from these studies clearly show selective trafficking of luciferase-expressing cells to the inflamed colon 4 h post-cell transfer with a significant reduction in neutrophil trafficking in the anti-KC-treated DSS mice.

Materials and methods

Mice

Male and female wild-type (wt) FVB/N mice, 8–12 weeks old, were obtained from Harlan (Oxon, UK). The β-actin/luciferase expressing (*luc*$^+$) transgenic FVB/N mice were purchased from Caliper Life Sciences (Alameda, CA, USA). All mice were housed individually and in a conventional environment (temperature 21°C, 12 h light : 12 h dark, humidity 50%) in a dedicated animal-holding facility. They were fed a standard non-sterile pellet diet and tap water *ad libitum*. Mice were allowed ≥2 weeks to acclimatise before entering the study. All animal procedures were performed according to national ethical guidelines.

Colitis induction and assessment: DSS model

For the bioluminescence imaging studies, acute colitis was induced in the recipient wild-type FVB/N mice by administering 4% DSS (47 kDa; TdB Consultancy, Uppsala, Sweden) in drinking water. The mice were exposed to DSS for 5 days followed by 1 day on tap water. DSS was changed once during the 5 days. Disease progression was assessed by monitoring body weight loss, stool consistency (0 = normal, well-formed pellets, 1 = changed formed pellets, 2 = loose stool, 3 = diarrhoea) and fur texture/posture (0 = smooth coat/not hunched, 1 = mildly scruffy/mildly hunched, 2 = very scruffy/very hunched), which were recorded to generate a daily disease activity index (DDAI). Distal colonic tissue samples were collected, weighed and homogenised in 50 ml phosphate-buffered saline (PBS) + 2 protease inhibitor cocktail tablets (Roche Applied Science, West Sussex, UK) + 10% fetal calf serum (FCS; Gibco, Paisley, UK). Homogenates were centrifuged for 12 min at 20 000 *g* at 4°C. Chemokine and cytokine levels were measured in the supernatants using a Meso Scale Discovery (MSD) 96-well mouse proinflammatory 7 plex kit and the electrochemiluminescent multiplex system Sector 2400 imager (Meso Scale Discovery, Gaithersburg, MD, USA), as per the manufacturer's instructions.

Induction of peritonitis and isolation of luc$^+$ donor neutrophils

Peritoneal exudate cells are primed, highly chemotactic and more functionally responsive in comparison to blood PMN leucocytes [20]. Thus, we chose to isolate these cells for both the *in vitro* and *in vivo* studies. Localised inflammation was induced in the peritoneal cavity of mice by intraperitoneal (i.p.) injection of 4% thioglycollate (Difco, Detroit, MI, USA) broth that had been previously autoclaved and stored at 4°C. Approximately 12 h later, a peritoneal lavage was performed on the mice following killing by decapitation. Briefly, 5 ml of harvest medium [1 × sterile Ca^{2+}/Mg^{2+}-free PBS (pH 7·2; Gibco) supplemented with 0·02% ethylenediamine tetraacetic acid (EDTA; Sigma-Aldrich, Dublin, Ireland) and 0·5% heat-inactivated FCS (Gibco)] was injected into the peritoneal cavity. The peritoneal wall was then massaged gently and the fluid withdrawn. This was repeated twice with 80–90% recovery of the lavage fluid. The lavage fluid was pooled and centrifuged at 300 ***g*** for 10 min at 25°C to recover leucocytes. The lavage solution was washed twice by resuspending in 10 ml sterile PBS (Gibco) and centrifuging at 300 ***g*** for 10 min. Leucocytes were counted using a haemocytometer. Approximately 5×10^6 cells per mouse were harvested.

Phenotypic characterisation of the peritoneal exudate using fluorescence activated cell sorter (FACS) analysis

Peritoneal exudate cells from three wild-type FVB/N mice were isolated and pooled as described above and resuspended at 1×10^6 cells/ml. To this cell suspension, 50 µl of each monoclonal antibody (mAb) dye mix was added with incubation in the dark at 4°C for 30 min. The mAbs used for flow cytometry included: anti-CD11c [immunoglobulin (Ig)G1], phycoerythrin cyanine dye 7 (PE-Cy7), HL3, anti-Ly6G (IgG2b), PE RB6-8C5, anti-CD4 (IgG2a), PE RM4-5, anti-CD49b (IgM) fluorescein isothiocyanate (FITC) DX5 (all from BD Pharmingen, Oxford, UK), anti-F4/80 (IgG2b) Tri-Color BM8 (Caltag, Buckingham, UK), anti-CD8 (IgG1) PE, anti-CD3 (IgG2B) FITC, anti-CXCR2 (IgG2a) allophycocyanin (APC) (R&D Systems, Abingdon, UK) and anti-B220 (IgG2a) Alexafluor (AF) 700 RA3-6B2 (Serotec, Kidlington, UK). For analysis of activation marker expression the mAbs

used were anti-CD11b (IgG2b), FITC MI/70 and anti-CD69 (IgG1) PE-Cy7 H1·2F3 (BD Pharmingen). Following staining, the cells were washed twice with blocking buffer [PBS + 1% bovine serum albumin (BSA; Sigma-Aldrich) + 1% rat serum (Sigma-Aldrich) + 1% hamster serum (Sigma-Aldrich) + 1% mouse serum (Dako Diagnostics, Dublin, Ireland) + 0·1% sodium azide (Sigma-Aldrich)] and fixed in 3% formalin for analysis. Relative fluorescence intensities were measured using a LSRII cytometer and BD Diva software (Becton Dickinson, Oxford, UK). For each sample, 20 000 events were recorded. The percentage of cells labelled with each mAb was calculated in comparison with cells stained with isotype control antibody. Background staining was controlled by labelled isotype controls (BD Biosciences, Caltag and Serotec) and fluorescence minus one (FMO). The results represent the percentage of positively stained cells in the total cell population exceeding the background staining signal.

Transwell™ *in vitro* chemotaxis assay

To analyse the functional migration activity of the peritoneal exudate cells towards recombinant KC in the presence or absence of an anti-KC antibody, a 96-well Neuroprobe ChemoTx Chemotaxis plate (Receptor Technologies, Adderbury, UK) with 5 μm pore polycarbonate filters was used, as described previously [21]. Peritoneal exudates from wild-type FVB/N mice were obtained by peritoneal lavage 12 h post-4% thioglycollate injection, and resuspended at a concentration of 8×10^6 cells/ml in serum-free RPMI-1640 media. The chemotactic factor murine recombinant (mr)KC (Peprotech, London, UK), diluted in serum-free RPMI-1640 to 10 ng/ml and with or without 0·1 μg/ml or 10 μg/ml monoclonal anti-mouse CXCL1/KC antibody (R&D Systems) was added to the lower chamber. Following placement of the filter membrane over the lower wells, 25 μl cells (2×10^5) were added to the upper chamber of each well. The plate was incubated for 4 h at 37°C with 5% CO_2. Inserts were removed, and the number of neutrophils that migrated into the bottom chamber was determined by counting using a haemocytometer and trypan blue. For each experiment, the % migration after subtraction of the control (RPMI medium alone) was given for KC alone (no anti-KC) and for two concentrations of anti-KC antibody.

Bioluminescence neutrophil trafficking model

To establish an efficient model to track and quantify neutrophil migration, we developed a neutrophil trafficking model using a *luc*$^+$ transgenic donor mouse line in conjunction with bioluminescent imaging. Expression of the luciferase reporter gene is detectable in all tissues including white blood cells of the transgenic β-actin-*luc*$^+$ mice. It has been demonstrated that *luc*$^+$ cells emit visible light photons that penetrate tissues and are detectable externally and quantitatively with high sensitivity [22]. Thus, 4×10^6 *luc*$^+$ donor neutrophils were adoptively transferred intravenously (i.v.) via the tail-vein of wild-type FVB/N recipients with DSS-induced colitis. Naive wild-type FVB/N mice with or without transferred *luc*$^+$ donor neutrophils were included as appropriate control groups. Bioluminescence imaging was performed as described previously [23], using an *IVIS* 100 charge-coupled device (CCD) imaging system (Xenogen, Alameda, CA, USA) at 2, 4, 16–22 h post-adoptive cell transfer. Briefly, the recipient mice were injected i.p. with the exogenous substrate D-luciferin (120 mg/kg body weight) (BioThema AB, Handen, Sweden) following gaseous anaesthesia with isoflurane, and transferred to the imaging chamber. Emission images were collected with 2 min integration times. Following the whole-body bioluminescent imaging, the mice were injected with an additional dose of D-luciferin. Five minutes later, the mice were killed and the organs were removed and imaged for 2 min. The bioluminescent signal was quantified by creation of regions of interest (ROIs). To standardise the data, light emission was quantified from the same surface area (ROI) for each organ type. In addition, background light emission, taken from ROIs created on organs of non-recipient non-DSS control animals, was subtracted from test organs. Imaging data were analysed and quantified with Living Image Software (Xenogen) and expressed as photons/s/cm^2.

Use of the model to show inhibition of neutrophil infiltration into inflamed tissue by anti-KC

DSS recipient mice (three and five, respectively) received purified isotype control rat IgG2aκ (BD Pharmingen) or a monoclonal rat anti-mouse CXCL1/KC antibody (R&D Systems) at a concentration of 20 μg/mouse i.p., 1 h pre-adoptive transfer of the *luc*$^+$ peritoneal neutrophils. Four h post-adoptive cell transfer, whole-body and *ex vivo* bioluminescent organ imaging was carried out in the same manner as described above.

Statistics

Data are expressed as means ± standard error of the mean (s.e.m.) unless stated otherwise. Statistical significance was determined with the unpaired Student's *t*-test using commercially available statistic software (GraphPad Software, San Diego, CA, USA). *P*-values <0·05 were considered statistically significant ($^*P < 0{\cdot}05$, $^{**}P < 0{\cdot}01$, $^{***}P < 0{\cdot}001$).

Results

Phenotypic characterisation of the peritoneal exudate

To determine neutrophil purity and the overall phenotype profile of the peritoneal exudate cells 12 h post-thioglycollate-induction of peritonitis, immunofluorescence flow cytometry was performed. The data revealed a neutro-

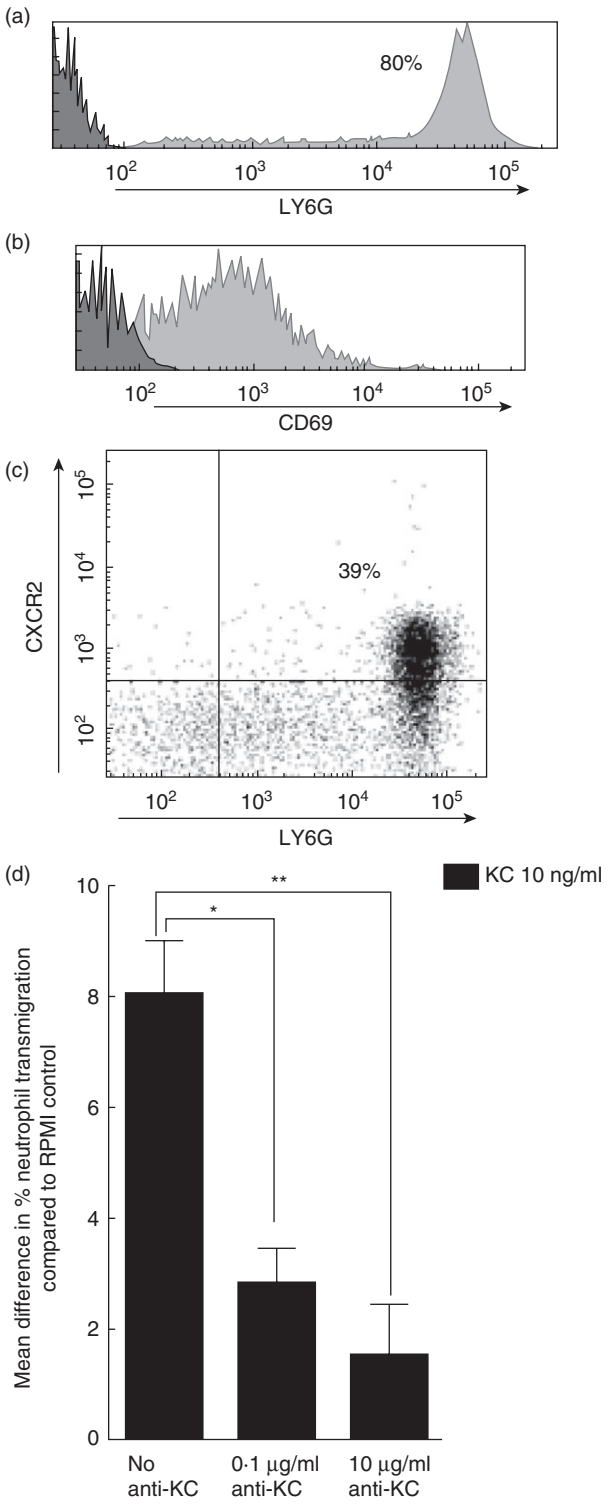

Fig. 1. Phenotypic and functional characterisation of the peritoneal exudate population. Cells were isolated from the peritoneum of FVB/N mice 12 h after intraperitoneal (i.p.) injection with thioglycollate. For the phenotypic analysis, single cell suspensions were stained with fluorochrome-labelled monoclonal antibodies (mAbs) and analysed by flow cytometry in which 20 000 events were recorded. (a) Percentage of neutrophils (i.e. Ly-6G$^+$ cells, grey area) present in the peritoneal exudate compared to isotype control antibody (black area). (b) Activation status of the neutrophils using anti-CD69 mAb (grey area) or isotype control antibody (black area). (c) Percentage of the Ly-6G$^+$ neutrophils that were CXCR2$^+$. Plots shown are representative of five independent experiments. (d) *In vitro* chemotaxis assay in which migrated cells from triplicate wells of the lower chambers were pooled and counted in trypan blue. For each experiment, the % migration after subtraction of the control (medium alone) was given for keratinocyte-derived chemokine (KC) (alone, no anti-KC) and for two concentrations of anti-KC antibody (0·1 μg/ml and 10 μg/ml), 4 h post-incubation at 37°C. Plots shown represent the mean of three independent experiments using pooled cell populations from three to six mice each time; $^*P \leq 0{\cdot}05$, $^{**}P < 0{\cdot}01$.

phil purity of 80%, i.e. LY6G$^+$ cells (Fig. 1a), with clear expression of the activation molecule CD69 on these neutrophils as shown by mean fluorescence intensity (Fig. 1b). CXCR2, the major receptor for human IL-8 and the murine homologues KC and MIP-2, was expressed on 39% of the neutrophils (Fig. 1c). We were unable to evaluate the expression of CXCR1 on these neutrophils due to a lack of commercially available antibody for flow cytometry, but it is likely that the remainder of the population are CXCR1-positive. Indeed, published studies have documented a similar CXCR1 and CXCR2 expression profile on human neutrophils [24]. Thus, the high percentage of activated neutrophils in the peritoneal exudate population demonstrates that these are suitable for adoptive transfer and neutrophil trafficking studies. The remaining 20% of the exudate consisted of 10% T (CD3$^+$) and B (B220$^+$) lymphocytes, with the rest being macrophages (F4/80$^+$), natural killer (NK) cells (DX5$^+$) and dendritic cells (CD11c$^+$) (data not shown). From previous studies we know that these cell numbers are too low to visualise using this bioluminescence model; thus, the luciferase-expressing cells visible in the recipient animals should be neutrophils.

Functional evaluation of *in vitro* chemotaxis

To confirm the chemotactic capability of the peritoneal exudate cells, an *in vitro* transwell system was used. Addition of mrKC to the bottom chamber of a 96-well Neuroprobe Chemotx plate induced mobilisation of peritoneal exudate neutrophils from the upper chamber. This migration was reduced by two different concentrations of anti-KC. In the presence of mrKC, there was an 8% increase in % neutrophil transmigration compared to the RPMI medium control, and this value was decreased to 2·8% and 1·5% by 0·1 μg/ml and 10 μg/ml anti-KC, respectively (Fig. 1d). This chemotaxis assay confirmed the suitability of the peritoneal exudate cells for adoptive transfer. Neutrophil migration towards recombinant MIP-2 instead of mrKC was also tested with similar results (data not shown).

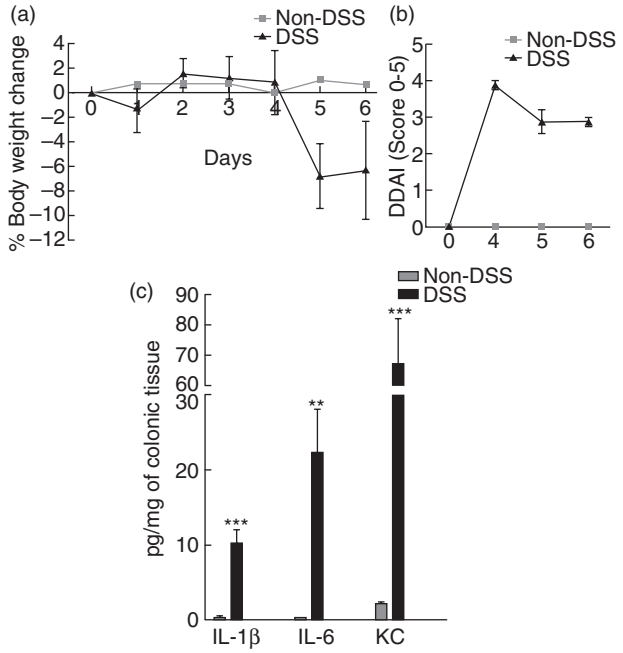

Fig. 2. Inflammation markers in dextran sodium sulphate (DSS)-induced colitis in FVB/N mice. (a) Mean % body weight changes in wild-type FVB/N mice from day 0 of treatment with 4% (w/v) DSS in drinking water for 5 days followed by 1 day of water. (b) Stool consistency and fur texture/posture were used to generate a daily disease activity index (DDAI). DSS-treated groups $n = 4$ and non-DSS control $n = 1$. (c) Treatment with DSS significantly increased KC levels and levels of the proinflammatory cytokines interleukin (IL)-1β and IL-6 in the distal colons of the mice; $n = 5$–6 per group; $^{**}P < 0{\cdot}01$, $^{***}P < 0{\cdot}001$. Plots shown are representative of five independent experiments.

Kinetic analysis of neutrophil trafficking in DSS-induced colitis

In the absence of inflammation, neutrophils (activated and responsive to KC) did not migrate to the colons of naive mice, indicating the necessity for localised gastrointestinal inflammation (Figs 4 and 5). Acute DSS colitis was therefore induced in recipient mice. Inflammation was confirmed by assessing body weight change and total DDAI (Fig. 2a and b), and by the significant increases in levels of KC and the proinflammatory cytokines IL-1β and IL-6 in the distal colons of the DSS mice, as reported previously [15,25] (Fig. 2c). In addition, we and others have provided both histological and myeloperoxidase (MPO) data confirming the colonic tissue damage caused by DSS administration [26–30]. Following induction of colitis, the temporal recruitment of neutrophils in living animals was analysed by performing whole-body and *ex vivo* organ bioluminescence imaging at 2, 4 and 16–22 h following adoptive transfer of *luc*$^+$ peritoneal exudate cells. Whole-body imaging confirmed presence of transferred viable neutrophils in recipient mice at all time-points (data not shown). At the early time-points of 2 and 4 h post-adoptive cell transfer, *ex vivo* imaging of organs revealed high neutrophil infiltration, as measured by bioluminescent signal in the lungs, spleens and livers of recipient DSS mice (Fig. 3c–e). The neutrophil signal in the colon was increased by 93% at 4 h compared to 2 h (Fig. 3a). At the later time-point of 16–22 h neutrophil presence in the colon remained high (Fig. 3a), but had decreased in the spleen, liver and lungs (Fig. 3c–e). Thus, the data show a robust signal in the inflamed colon at all time-points post-cell transfer. There was no evidence of neutrophil recruitment to the small intestines of DSS recipient mice at any of the time-points studied (data not shown).

Effects of KC blockade on neutrophil influx during DSS-induced colitis

To illustrate the potential of the bioluminescence neutrophil trafficking model, we assessed the effect of a chemokine blocking antibody, anti-KC. Four hours post-adoptive transfer of *luc*$^+$ neutrophils from transgenic donors, a clear bioluminescent signal was apparent in the whole-body images of all the recipient DSS mice and of the naive control mice, in contrast to the non-recipient non-DSS control, specifically in the upper part of the body and in the inguinal lymph nodes (Fig. 4a). These images confirm that the recipient mice received viable luciferase-expressing cells that can be detected *in vivo*. However, as some attenuation of optical signal is expected to occur with tissue depth, *ex vivo* imaging of the organs is necessary for accurate visualisation and quantitation of neutrophil localisation.

Ex vivo imaging of the organs revealed high neutrophil presence (i.e. bioluminescent signal) in the spleens and lungs of the IgG control-treated and anti-KC-treated DSS recipients, confirming our observations from the whole-body imaging. There was no significant increase or decrease in neutrophil recruitment to liver, spleen or lungs in the anti-KC treated group compared to the IgG control-treated group (Fig. 5b). However, a significant reduction in the signal from the colons of the DSS-recipients that were treated with anti-KC compared to the IgG control-treated recipients was observed (Figs 4b and 5a). Similar to the kinetic study, no bioluminescence signal was evident in the small intestines of both IgG control-treated and anti-KC treated groups (data not shown). In the naive recipients, i.e. the control group, there was significantly higher localisation of neutrophils in the liver, spleen and lungs compared to the DSS recipient mice (Fig. 5b). However, in contrast to the DSS recipients, there was no bioluminescence signal evident in the naive colons (Fig. 5a).

Discussion

In both human and experimental IBD, PMN invasion of the intestinal lamina propria and crypts correlates with tissue damage and clinical symptoms, suggesting that targeting

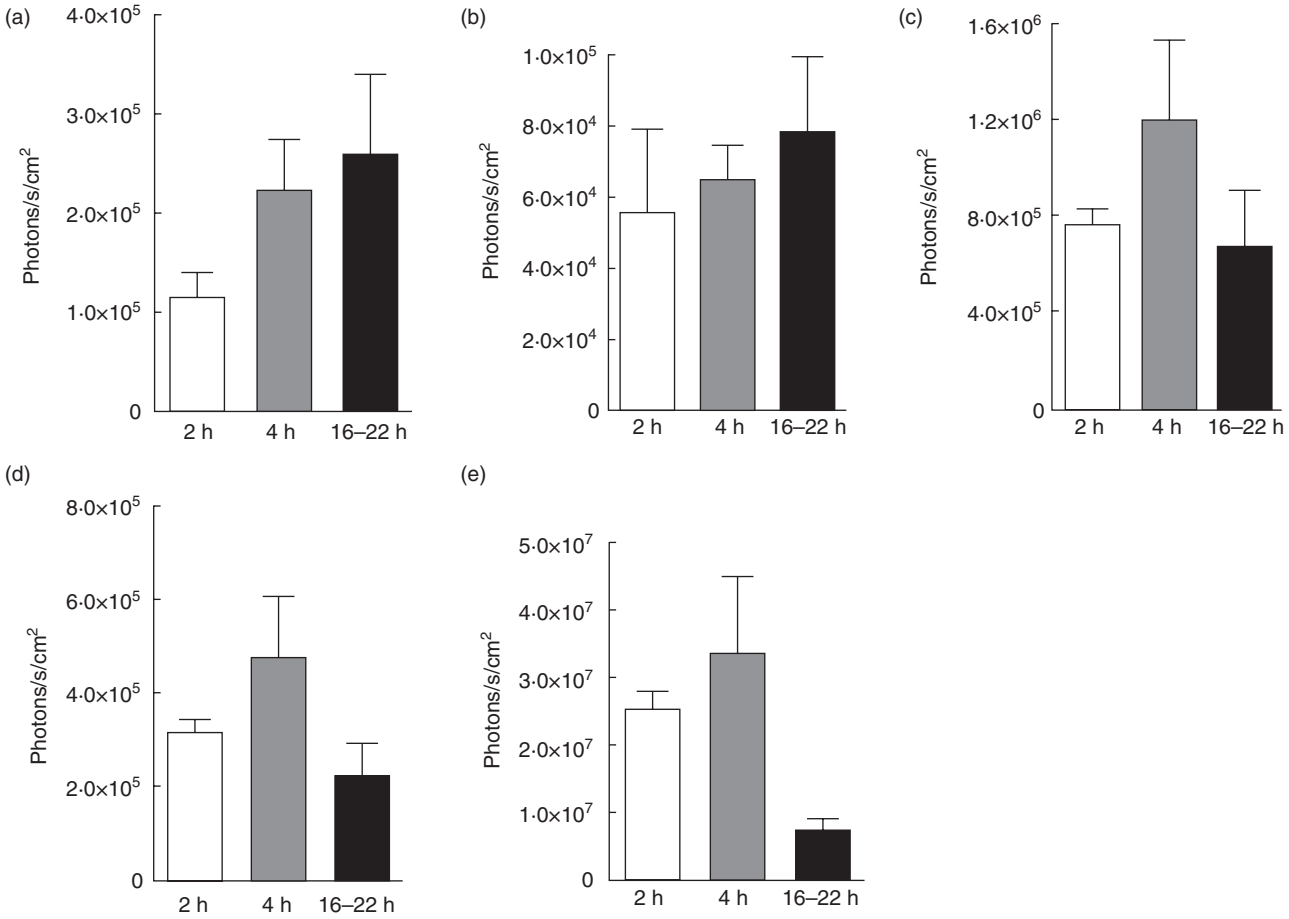

Fig. 3. Kinetic analysis of neutrophil trafficking *in vivo*. Bioluminescent signal in organs dissected from dextran sodium sulphate (DSS) recipient mice at 2, 4 and 16–22 h post-adoptive transfer with *luc*$^+$ exudate cells. Neutrophil trafficking kinetics to (a) colon, (b) mesenteric lymph nodes (MLNs), (c) spleen, (d) liver and (e) lungs are shown. DSS-treated groups; $n = 5$–8. Plots shown are representative of two independent experiments and the mean values are indicated.

neutrophil recruitment is a viable therapeutic strategy for IBD. This study presents a robust model to analyse the biology of neutrophil trafficking that can also be used in preclinical studies to evaluate new therapeutic compounds aimed specifically at blocking neutrophil recruitment. The first step in developing the model was to characterise the purity and functional properties of the neutrophil population from thioglycollate-induced peritonitis. Phenotypic analysis of the peritoneal exudate isolated 12 h post-i.p. administration of thioglycollate, revealed 80% neutrophil purity. In addition, the cells were activated and functionally responsive to recombinant KC *in vitro*, and their chemotaxis was inhibited by the presence of an anti-KC antibody. These results showed that the post-thioglycollate peritoneal exudate population of neutrophils was appropriate for the adoptive transfer model.

Bioluminescence imaging of whole-body and *ex vivo* organs was used to track and quantify neutrophil trafficking following adoptive transfer of *luc*$^+$ peritoneal exudate cells from transgenic donors. This is a non-invasive technology allowing real-time detection of tagged cells *in vivo* using CCD cameras due to the detection of visible light produced by luciferase-catalysed reactions [31]. In contrast to other imaging modalities, such as positron emission tomography (PET), single photon emission computed tomography (SPECT) and magnetic resonance imaging (MRI), bioluminescence imaging is less complicated, less labour-intensive and relatively low cost while still providing quantitative, spatial and temporal data. In addition, bioluminescence overcomes the problems encountered commonly with using fluorescent labels such as carboxyfluorescein succinimidyl ester (CFSE) and green fluorescent protein (GFP), namely the exponentially decreasing light intensity with tissue depth and the limited sensitivity and specificity as a result of endogenous tissue autofluorescence [32,33]. So far, bioluminescence has been used to monitor infection progression, transgene expression, tumour growth and metastasis, transplantation, toxicology and gene therapy [31]. In the context of cell tracking, Sheikh *et al.* successfully used bioluminescence imaging to track bone marrow mononuclear cell

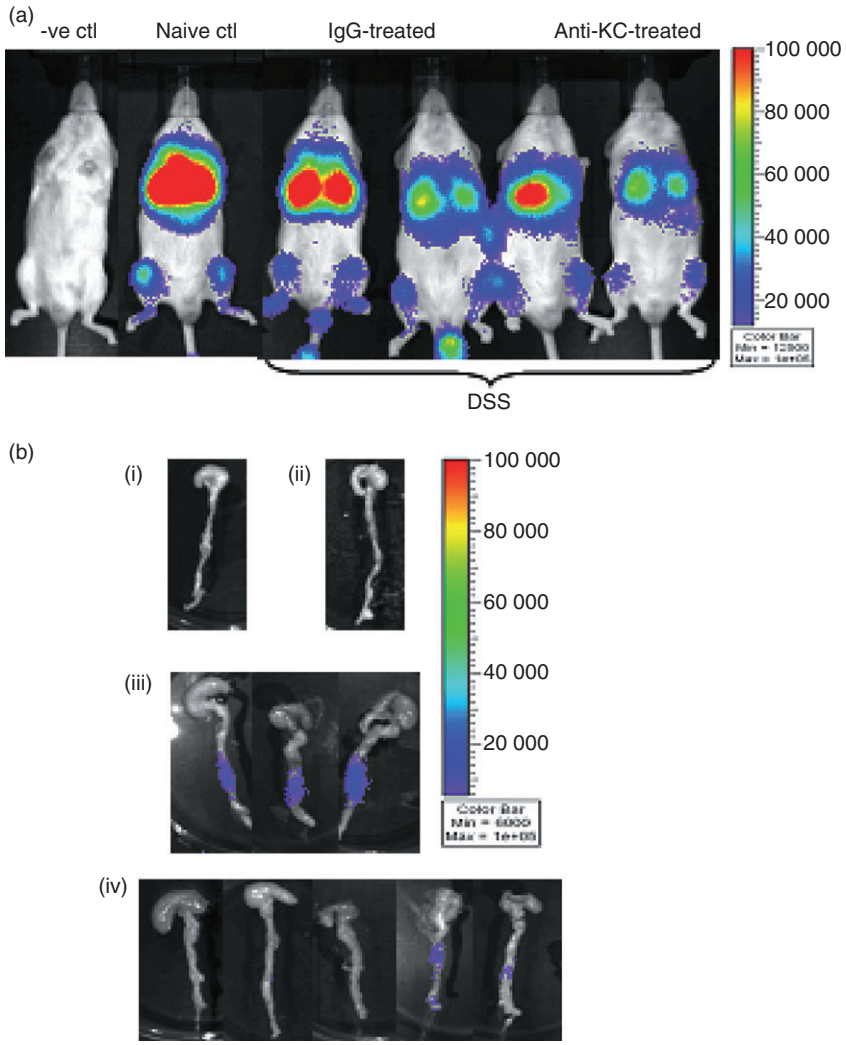

Fig. 4. Effect of anti-mouse KC on neutrophil trafficking. (a). Representative whole body bioluminescence images of wt FVB/N recipients with dextran sodium sulphate (DSS)-induced colitis treated with isotype control rat immunoglobulin (Ig)G2a or anti-keratinocyte-derived chemokine (KC) antibody, 4 h post-adoptive transfer with *luc*$^+$ cells. Non-DSS/naive recipients were also included as a control group. (b) *Ex vivo* images of colon of (i) non-DSS non-recipient negative control, (ii) non-DSS/naive recipient mouse and DSS recipient mice treated with (iii) IgG control or (iv) anti-KC (20 μg/mouse). Non-DSS/naive recipient, non-DSS-treated and DSS-treated groups; $n = 3–5$.

homing in ischaemic myocardium [34], while Costa *et al*. used a retroviral vector containing luciferase and GFP to illuminate the migratory patterns of CD4$^+$ T cells in a mouse model of multiple sclerosis [35]. These and other studies have shown robust correlation between cell numbers and bioluminescence signals [23]. The results of the present study demonstrated that the adoptively transferred neutrophils migrated preferentially to the diseased sites in the recipient animals with DSS-induced colitis, with high infiltration of the colon at all time-points investigated. In contrast, high transit through the lungs and spleen was evident at early time-points following cell transfer but declined at the later time-point. This is due probably to redirection of the transferred neutrophils to the inflamed colon with return to basal conditions in these organs. While it is also possible that this reduction in signal is due to a decrease in overall viability of transferred circulatory neutrophils we think this to be unlikely, as signal in the colon is observed to increase at these later time-points. Additionally, neutrophil half-life in tissues is 1–2 days and the latest time-point in our study was less than that at 22 h [36]. Because the route of administration of the donor cells was intravenous (i.v.), neutrophil localisation to the lungs, liver and spleen of the recipient mice reflects the natural route of circulation. In fact, it is possible that the higher neutrophil presence in the inflamed colon at the later time-points of 4 h and 16–22 h compared to 2 h post-adoptive transfer of cells is due to the fact that a recovery time of at least 2 h is necessary to allow transferred cells to equilibrate in the circulation following i.v. administration. There was significantly higher neutrophil presence in the lungs, liver and spleen of the naive recipients compared to the DSS recipients, which was due most probably to the absence of gut inflammation. Similar findings have been noted in previous studies, where neutrophil presence in the spleen declined in patients with severe inflammatory disease compared to normal subjects, the explanation for this being that the pooled cells had been redirected to inflammatory foci [37,38]. In addition, we investigated the utility of the bioluminescence model as a tool to dissect the biology of and test new drugs that target neutrophil migration using a blocking antibody against KC. Significant inhibition of neutrophil recruitment to the inflamed colons of the anti-KC-

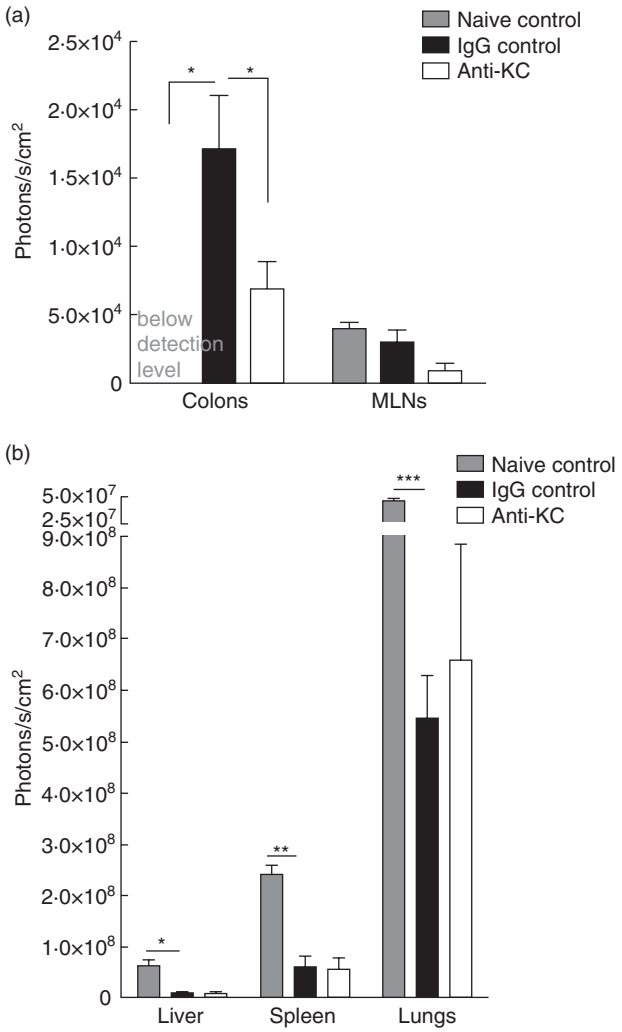

Fig. 5. Anti-keratinocyte-derived chemokine (KC) administration markedly reduced neutrophil trafficking to the colons of mice with dextran sodium sulphate (DSS)-induced colitis. Summary of bioluminescent signal in (a) colon and mesenteric lymph nodes (MLNs) and (b) liver, spleen and lungs dissected from naive controls and DSS mice treated with immunoglobulin (Ig)G control or anti-KC antibody, 4 h post-adoptive transfer with *luc*$^+$ cells. Mean signal from the colons of naive recipients was below the background light emission from the non-recipient control colons. $P \leq 0{\cdot}05$; $n = 3$–5 per group. Plots shown are representative of two independent experiments.

treated mice compared to IgG control-treated was clearly evident using this system. Interestingly, it has been reported that treatment of mice with trinitrobenzene sulphonic acid (TNBS)-induced colitis with anti-KC ameliorated disease by reducing neutrophil migration and MPO [39].

The bioluminescence model presented here has definite and distinct advantages over other *ex vivo* techniques used to track neutrophil recruitment. First and foremost, the necessity for pre-labelling of cells is removed, as the donor cells used constitutively express luciferase. This eliminates the common problems associated with cell-labelling, such as alteration of cellular functions, variable labelling efficiency and elution of label from the cells of interest. In addition, our technique allows direct *ex vivo* visualisation without any need for further processing of the tissues, in contrast to immunohistochemistry and MPO analysis. Histology is labour-intensive and tedious, while MPO assays can be problematic and do not distinguish between neutrophils and macrophages.

In conclusion, this study presents a robust model to track neutrophil recruitment which can be used to complement other available methods traditionally used for tracking neutrophils. In addition to experimental models of IBD, this versatile technique will be useful for monitoring neutrophil trafficking during inflammatory responses in a range of disease settings and constitutes a novel approach for the assessment of potential therapeutics that aim to reduce neutrophil infiltration. Thus, it can be used as an informative and specific tool for both the pharmaceutical industry and the basic research community.

Acknowledgements

We thank Grainne Hurley for her excellent technical assistance. The authors are supported in part by Science Foundation Ireland and by a research grant from GlaxoSmithKline.

Disclosure

None of the co-authors have any conflict of interest to declare in connection to the paper. The work described has not been published or submitted elsewhere. S.M. and G.M. are employees of GlaxoSmithKline.

References

1 Nathan C. Neutrophils and immunity: challenges and opportunities. Nat Rev Immunol 2006; **6**:173–82.
2 Diamanti A, Colistro F, Basso MS *et al.* Clinical role of calprotectin assay in determining histological relapses in children affected by inflammatory bowel diseases. Inflamm Bowel Dis 2008; **14**:1229–35.
3 Kobayashi Y. Neutrophil infiltration and chemokines. Crit Rev Immunol 2006; **26**:307–16.
4 Matityahu E, Feniger-Barish R, Meshel T, Zaslaver A, Ben-Baruch A. Intracellular trafficking of human CXCR1 and CXCR2: regulation by receptor domains and actin-related kinases. Eur J Immunol 2002; **32**:3525–35.
5 Podolin PL, Bolognese BJ, Foley JJ *et al.* A potent and selective nonpeptide antagonist of CXCR2 inhibits acute and chronic models of arthritis in the rabbit. J Immunol 2002; **169**:6435–44.
6 Schuh JM, Blease K, Hogaboam CM. CXCR2 is necessary for the development and persistence of chronic fungal asthma in mice. J Immunol 2002; **168**:1447–56.
7 Belperio JA, Keane MP, Burdick MD *et al.* Critical role for CXCR2

and CXCR2 ligands during the pathogenesis of ventilator-induced lung injury. J Clin Invest 2002; **110**:1703–16.
8 Buanne P, Di Carlo E, Caputi L *et al*. Crucial pathophysiological role of CXCR2 in experimental ulcerative colitis in mice. J Leukoc Biol 2007; **82**:1239–46.
9 Banks C, Bateman A, Payne R, Johnson P, Sheron N. Chemokine expression in IBD. mucosal chemokine expression is unselectively increased in both ulcerative colitis and Crohn's disease. J Pathol 2003; **199**:28–35.
10 Daig R, Andus T, Aschenbrenner E, Falk W, Scholmerich J, Gross V. Increased interleukin 8 expression in the colon mucosa of patients with inflammatory bowel disease. Gut 1996; **38**:216–22.
11 Mazzucchelli L, Hauser C, Zgraggen K *et al*. Expression of interleukin-8 gene in inflammatory bowel disease is related to the histological grade of active inflammation. Am J Pathol 1994; **144**:997–1007.
12 Autschbach F, Giese T, Gassler N *et al*. Cytokine/chemokine messenger-RNA expression profiles in ulcerative colitis and Crohn's disease. Virchows Arch 2002; **441**:500–13.
13 McColl SR, Clark-Lewis I. Inhibition of murine neutrophil recruitment *in vivo* by CXC chemokine receptor antagonists. J Immunol 1999; **163**:2829–35.
14 Roche JK, Keepers TR, Gross LK, Seaner RM, Obrig TG. CXCL1/KC and CXCL2/MIP-2 are critical effectors and potential targets for therapy of *Escherichia coli* O157:H7-associated renal inflammation. Am J Pathol 2007; **170**:526–37.
15 Melgar S, Drmotova M, Rehnstrom E, Jansson L, Michaelsson E. Local production of chemokines and prostaglandin E2 in the acute, chronic and recovery phase of murine experimental colitis. Cytokine 2006; **35**:275–83.
16 Lowell CA, Berton G. Resistance to endotoxic shock and reduced neutrophil migration in mice deficient for the Src-family kinases Hck and Fgr. Proc Natl Acad Sci USA 1998; **95**:7580–4.
17 Bennink RJ, Hamann J, de Bruin K, ten Kate FJ, van Deventer SJ, te Velde AA. Dedicated pinhole SPECT of intestinal neutrophil recruitment in a mouse model of dextran sulfate sodium-induced colitis. J Nucl Med 2005; **46**:526–31.
18 Bennink RJ, Peeters M, Rutgeerts P, Mortelmans L. Evaluation of early treatment response and predicting the need for colectomy in active ulcerative colitis with 99mTc-HMPAO white blood cell scintigraphy. J Nucl Med 2004; **45**:1698–704.
19 Parish CR. Fluorescent dyes for lymphocyte migration and proliferation studies. Immunol Cell Biol 1999; **77**:499–508.
20 Zimmerli W, Seligmann B, Gallin JI. Exudation primes human and guinea pig neutrophils for subsequent responsiveness to the chemotactic peptide N-formylmethionylleucylphenylalanine and increases complement component C3bi receptor expression. J Clin Invest 1986; **77**:925–33.
21 Frevert CW, Wong VA, Goodman RB, Goodwin R, Martin TR. Rapid fluorescence-based measurement of neutrophil migration *in vitro*. J Immunol Methods 1998; **213**:41–52.
22 Sweeney TJ, Mailander V, Tucker AA *et al*. Visualizing the kinetics of tumor-cell clearance in living animals. Proc Natl Acad Sci USA 1999; **96**:12044–9.
23 Edinger M, Hoffmann P, Contag CH, Negrin RS. Evaluation of effector cell fate and function by *in vivo* bioluminescence imaging. Methods 2003; **31**:172–9.
24 Cummings CJ, Martin TR, Frevert CW *et al*. Expression and function of the chemokine receptors CXCR1 and CXCR2 in sepsis. J Immunol 1999; **162**:2341–6.
25 Alex P, Zachos NC, Nguyen T *et al*. Distinct cytokine patterns identified from multiplex profiles of murine DSS and TNBS-induced colitis. Inflamm Bowel Dis 2008; **15**:341–52.
26 Melgar S, Karlsson A, Michaelsson E. Acute colitis induced by dextran sulfate sodium progresses to chronicity in C57BL/6 but not in BALB/c mice: correlation between symptoms and inflammation. Am J Physiol Gastrointest Liver Physiol 2005; **288**:G1328–38.
27 Wirtz S, Neufert C, Weigmann B, Neurath MF. Chemically induced mouse models of intestinal inflammation. Nat Protoc 2007; **2**:541–6.
28 Cooper HS, Murthy SN, Shah RS, Sedergran DJ. Clinicopathologic study of dextran sulfate sodium experimental murine colitis. Lab Invest 1993; **69**:238–49.
29 Okayasu I, Hatakeyama S, Yamada M, Ohkusa T, Inagaki Y, Nakaya R. A novel method in the induction of reliable experimental acute and chronic ulcerative colitis in mice. Gastroenterology 1990; **98**:694–702.
30 Krieglstein CF, Cerwinka WH, Laroux FS *et al*. Role of appendix and spleen in experimental colitis. J Surg Res 2001; **101**:166–75.
31 Sadikot RT, Blackwell TS. Bioluminescence imaging. Proc Am Thorac Soc 2005; **2**:537–40, 511–12.
32 Rice BW, Cable MD, Nelson MB. *In vivo* imaging of light-emitting probes. J Biomed Opt 2001; **6**:432–40.
33 Troy T, Jekic-McMullen D, Sambucetti L, Rice B. Quantitative comparison of the sensitivity of detection of fluorescent and bioluminescent reporters in animal models. Mol Imaging 2004; **3**:9–23.
34 Sheikh AY, Lin SA, Cao F *et al*. Molecular imaging of bone marrow mononuclear cell homing and engraftment in ischemic myocardium. Stem Cells 2007; **25**:2677–84.
35 Costa GL, Sandora MR, Nakajima A *et al*. Adoptive immunotherapy of experimental autoimmune encephalomyelitis via T cell delivery of the IL-12 p40 subunit. J Immunol 2001; **167**:2379–87.
36 Edwards SW, Moulding DA, Derouet M, Moots RJ. Regulation of neutrophil apoptosis. Chem Immunol Allergy 2003; **83**:204–24.
37 Saverymuttu SH, Peters AM, Keshavarzian A, Reavy HJ, Lavender JP. The kinetics of 111indium distribution following injection of 111indium labelled autologous granulocytes in man. Br J Haematol 1985; **61**:675–85.
38 Peters AM, Saverymuttu SH, Keshavarzian A, Bell RN, Lavender JP. Splenic pooling of granulocytes. Clin Sci (Lond) 1985; **68**:283–9.
39 Bento AF, Leite DF, Claudino RF, Hara DB, Leal PC, Calixto JB. The selective nonpeptide CXCR2 antagonist SB225002 ameliorates acute experimental colitis in mice. J Leukoc Biol 2008; **84**:1213–21.